Detection of Recurrent Prostate Cancer After Radical Prostatectomy: Comparison of ^{11}C-Choline PET/CT with Pelvic Multiparametric MR Imaging with Endorectal Coil

Kazuhiro Kitajima[1], Robert C. Murphy[1], Mark A. Nathan[1], Adam T. Froemming[1], Clinton E. Hagen[2], Naoki Takahashi[1], and Akira Kawashima[1]

[1]*Department of Radiology, Mayo Clinic, Rochester, Minnesota; and* [2]*Department of Biomedical Statistics and Informatics, Mayo Clinic, Rochester, Minnesota*

The aim of this study was to compare ^{11}C-choline PET/CT with pelvic multiparametric MR imaging for detection of recurrent prostate carcinoma in patients with suspected recurrence after radical prostatectomy and to identify an optimal imaging method to restage these patients. **Methods:** This was a retrospective, single-institution study of 115 prostatectomy patients with suspected tumor recurrence who underwent both ^{11}C-choline PET/CT and multiparametric MR imaging with endorectal coil. The reference standard included histopathology, treatment change, and imaging follow-up for determination of locally recurrent tumor, lymph node (LN) metastases, and skeletal metastases. Two nuclear medicine and 2 genitourinary radiologists independently and in a masked manner reviewed PET/CT and multiparametric MR imaging, respectively. The reviewers assessed for local recurrence in the prostatectomy bed as well as LN and bone metastases, rating their diagnostic confidence with a 5-point scoring system for each location. Receiver-operating-characteristic analysis was used to compare the 2 modalities. **Results:** The standard of reference (either positive or negative) for the diagnosis of local recurrence and pelvic LN and bone metastases was met in 87, 70, and 95 patients, respectively. Documented local recurrence and pelvic LN and bone metastases was present in 61 of 87 (70.1%), 50 of 70 (71.4%), and 16 of 95 (16.8%) patients, respectively. Patient-based area under the receiver-operating-characteristic curves of multiparametric MR imaging versus PET/CT for the diagnosis of local recurrence and pelvic LN and bone metastases were 0.909 versus 0.761 ($P = 0.0079$), 0.812 versus 0.952 ($P = 0.0064$), and 0.927 versus 0.898 ($P = 0.69$), respectively. Among 61 patients with local recurrence, 32 patients (52.4%) were correctly diagnosed as having local recurrence by both multiparametric MR imaging and PET/CT, 22 (36.1%) were correctly diagnosed by multiparametric MR imaging only, 6 (9.8%) could not be diagnosed by either modality, and 1 (1.6%) was correctly diagnosed by PET/CT only. The patient-based sensitivity, specificity, and accuracy of multiparametric MR imaging for diagnosing local recurrence were 88.5% (54/61), 84.6% (22/26), and 87.4% (76/87) whereas those of PET/CT for detecting body LN or bone metastases were 92.3% (72/78), 100% (18/18), and 93.8% (90/96), respectively. **Conclusion:** Multiparametric MR imaging with endorectal coil is superior for the detection of local recurrence, PET/CT is superior for pelvic LN metastasis, and both were equally excellent for pelvic bone metastasis. ^{11}C-choline PET/CT and pelvic multiparametric MR imaging are complementary for restaging prostatectomy patients with suspected recurrent disease.

Key Words: prostate cancer; prostatectomy; biochemical failure; ^{11}C-choline PET/CT; multiparametric MR imaging

J Nucl Med 2014; 55:223–232
DOI: 10.2967/jnumed.113.123018

Biochemical failure after radical prostatectomy (RP) is defined as a prostate-specific antigen (PSA) level of 0.2 ng/mL or greater followed by another increased value (*1*) and often precedes clinically detectable recurrence by years. In these patients, it is important to determine whether there is localized recurrent disease, metastases to lymph node (LN) or bone, or a combination of localized recurrent and metastatic disease. This determination affects subsequent management, such as consideration of salvage therapy for localized recurrence, systemic treatment for metastatic disease, or a combination of these.

CT, bone scintigraphy, and transrectal ultrasound–guided biopsy have been traditionally used to localize recurrent or metastatic disease although these examinations lack adequate sensitivity and accuracy. In recent years, PET/CT using ^{11}C- or ^{18}F-choline has emerged as a promising molecular imaging tool, providing a body examination in 1 step. Many researchers have reported the usefulness of ^{11}C-choline PET/CT for restaging prostate cancer after RP, especially for detecting distant metastases most commonly to LNs and bones (*2,3*). However, only limited data on the utility of ^{11}C-choline PET/CT regarding the detection of local recurrence after RP are available in the literature (*4,5*). Conversely, the combination of T2-weighted imaging and dynamic contrast-enhanced (DCE) MR imaging with endorectal coil has been shown to have an 84%–97% sensitivity and 74%–89% specificity for detecting local recurrence in the prostatectomy bed (*6–8*). However, the diagnostic performance of MR imaging for metastasis to pelvic LN and bone was not addressed in these studies.

There has been no report directly comparing the diagnostic capability of ^{11}C-choline PET/CT and multiparametric MR imaging with endorectal coil for the detection of both local recurrence in the prostatic fossa and metastasis to pelvic LN and bone after RP. One report has compared ^{18}F-choline PET/CT and endorectal coil, multiparametric MR imaging including DCE-MR imaging, and ^{1}H MR spectroscopic imaging for detecting local recurrence (*9*). However, ^{18}F-choline may be an inferior tracer for evaluating the pelvis in

Received Mar. 18, 2013; revision accepted Aug. 6, 2013.
For correspondence or reprints contact: Akira Kawashima, Department of Radiology, Mayo Clinic, 200 First St. SW, Rochester, MN 55905.
E-mail: kawashima.akira@mayo.edu
Published online Jan. 16, 2014.

comparison with ^{11}C-choline, especially in the prostate bed, because of the higher urinary excretion (*10*). In another study, diffusion-weighted MR imaging was shown to be equal to short-inversion-time inversion recovery and T1-weighted SE sequences and ^{11}C-choline PET/CT in detecting bone metastases from prostate cancer (*11*). However, only 11 patients were enrolled.

The purpose of our study was to directly compare ^{11}C-choline PET/CT with multiparametric MR imaging for detecting local recurrence and pelvic LN and bone metastases in patients with clinical suspicion of prostate cancer recurrence after RP and to identify an optimal imaging method to restage these patients.

MATERIALS AND METHODS

Patients

This was a Health Insurance Portability and Accountability Act of 1996–compliant, retrospective study conducted under the approval of the institutional review board, and the requirement to obtain informed consent was waived. From June 2009 to April 2012, 847 patients underwent pelvic multiparametric MR imaging with endorectal coil (n = 451 with 3.0-T MR imaging, n = 396 with 1.5-T MR imaging), and 342 patients underwent ^{11}C-choline PET/CT of the body for clinically suspected recurrence of prostate cancer after RP at our institution. Of these patients, 139 who underwent both PET/CT and MR imaging within 14 d of each other were identified. Twenty-four of the 139 patients were excluded because of insufficient clinical follow-up. The remaining 115 patients (mean age, 66 y; range, 49–87 y) constituted the final study population (Table 1). Fifteen patients were undergoing androgen-deprivation therapy at the time of the PET/CT examinations.

TABLE 1
Patient and Original Tumor Characteristics (n = 115)

Characteristic	Value
Age (y)	
Mean	65.7
Range	49–87
PSA level (ng/mL) at MR imaging/ ^{11}C-choline PET/CT	
Mean	5.26
Range	0.58–68.3
Median	2.5
Interval between RP and MR imaging/ ^{11}C-choline PET/CT (mos)	
Mean	80.8
Range	4–276
Treatment before MR imaging/ ^{11}C-choline PET/CT (%)	
RP only	30 (26.1)
RP and salvage EBRT	30 (26.1)
RP and ADT	29 (25.2)
RP, salvage EBRT, and ADT	25 (21.7)
RP, salvage cryoablation, and ADT	1 (0.9)
Pathologic stage at surgery (%)	
pT2 N0	41 (35.7)
pT3a N0	21 (18.3)
pT3b N0	21 (18.3)
Any T pN1	32 (27.8)
Positive surgical margin (%)	52 (45.2)
Pathologic Gleason scores at surgery (%)	
2–6	10 (8.7)
7 (3 + 4)	37 (32.2)
7 (4 + 3)	23 (20.0)
8–10	45 (39.1)

Values in parentheses are percentages.
EBRT = external-beam radiotherapy; ADT = androgen-deprivation therapy.

^{11}C-Choline PET/CT Technique

All PET/CT scans were obtained with either Discovery RX or Discovery 690 (GE Healthcare) dedicated PET/multislice CT scanners. The patients received an intravenous injection of ^{11}C-choline (370–555 MBq). The PET/CT scan started 5 min after the injection, and emission data were acquired at 7–8 bed positions proceeding from the proximal thighs to the base of the skull, taking 3 min (patient body mass index [BMI] $\leq$ 35 kg/cm^2) or 4 min (BMI $>$ 35 kg/cm^2) for each position in a 3-dimensional (3D) mode. PET images were corrected for random scatter, corrected for attenuation, and were reconstructed on a 128 (RX) or 192 (690) image matrix using an ordered-subsets expectation maximization algorithm (2 iterations, 35 subsets for RX; 2 iterations, 36 subsets for 690), followed by a postreconstruction smoothing gaussian filter (7 mm full width at half maximum for patients with BMI $\leq$ 35 kg/cm^2; 7.5 mm for patients with BMI $>$ 35 kg/cm^2). The low-dose CT parameters were 120 kVp, 20–160 mA (auto mA settings), 0.5 s per tube rotation, slice thickness of 3.75 mm, slice interval of 3.27 mm, pitch of 1.75 (RX) and 0.984 (690), and table speed of 17.5 mm/rotation (RX) and 39.4 mm/rotation (690).

MR Imaging Technique

Fifty-eight patients were examined using a 3-T MR scanner (MR750; GE Healthcare), and 57 patients with 1.5-T MR scanners (Signa; GE Healthcare). The integration of endorectal (Medrad) and pelvic phased-array coils was used with both units. The endorectal coil was insufflated with 50 mL of 60% w/v barium sulfate suspension (E-Z-EM).

Our institutional standard pelvic MR imaging protocol for evaluating locally recurrent prostate cancer is shown in Table 2. For DCE MR imaging acquisition, 3D fast gradient-echo axial images were acquired before and after administration of the contrast agent. Multiphase dynamic images were obtained every 40 s at 1.5-T or 30 s at 3.0-T for 5 min. Gadodiamide (0.08–0.1 mmol/kg, Omniscan; GE Healthcare) was administered at a rate of 2 mL/s, followed by a saline flush (15 mL at 2 mL/s) using the MR imaging–compatible mechanical power injector (Spectris; Medrad). Apparent diffusion coefficient maps were generated from diffusion-weighted MR imaging.

Determination of Reference Standard

The criteria for defining a true-positive MR imaging or PET/CT result included histopathologic findings obtained at subsequent biopsy or reduction in PSA level after salvage radiotherapy with respect to local recurrence, histopathologic findings obtained at subsequent surgical lymphadenectomy or biopsy with respect to LN metastases, histopathologic findings confirmed by biopsy or subsequent confirmation with dedicated CT or MR imaging with respect to skeletal metastases, and follow-up of greater than 6 mo (including pelvic MR imaging, CT, or PET/CT) revealing an increase in size of the suspected lesions or, alternatively, resolution or reduction in size of the suspected lesions associated with a normalization or reduction of PSA values with salvage therapy. The criteria for defining negative findings included negative histopathologic findings obtained by surgery or biopsy or negative follow-up of at least 12 mo with pelvic multiparametric MR imaging, ^{11}C-choline PET/CT, CT, or bone scintigraphy with no progression of PSA level.

Image Analysis

Two board-certified nuclear medicine radiologists with 7 and 5 y of ^{11}C-choline PET/CT experience, who were masked to the clinical and histopathologic information and other imaging examinations, retro-

TABLE 2
3- and 1.5-T Endorectal Coil MR Imaging Protocols

Sequence	Anatomic coverage	Imaging plane	Field of view (cm)	Repetition time/echo time (ms)	Slice thickness /gap or overlap (mm)	Matrix/no. of excitations	Flip angle (°)	*b* values (ms/mm^2)
3-T								
Precontrast imaging								
T1WI FSE	Entire pelvis	Axial	40 × 32–42 × 42	665–775/8.1	6/1 sp	320 × 192–224/1–2	90	
DWI spin-echo EPI	Entire pelvis	Axial	42 × 32–42 × 42	4,000/48–55.3	7/1 sp	128 × 192/6	90	0, 600
T2WI FRFSE	Prostatectomy bed	Axial, coronal, sagittal	16 × 16–18 × 18	5,500–7,600/98–109	2.5/0.5 sp	320–352 × 256/2–3	90	
DWI spin-echo EPI	Prostatectomy bed	Axial	22 × 22	4,000/64–66	5/1 sp	128–192 × 192/6	90	0, 600, 1,000
Dynamic gadolinium contrast-enhanced imaging								
LAVA 3D FSPGR	Prostatectomy bed	Axial	18 × 18	5.2–5.3/2.6	2.6/50 % overlap	320 × 192/0.71–0.73	12	
Post–gadolinium contrast-enhanced imaging								
LAVA Flex 3D FSPGR	Entire pelvis	Axial	38 × 30	4.1–4.2/1.8–1.9	4–5/50 % overlap	320 × 224/0.69–070	12	
1.5-T								
Precontrast imaging								
T1WI FSE	Entire pelvis	Axial	36 × 36	533–600/8.4–8.7	6/1 sp	320 × 256/2	90	
DWI spin echo EPI	Entire pelvis	Axial	35 × 35–40 × 40	4,000/45–48	8/2 sp	128 × 128/2		0, 600
T2WI FRFSE	Prostatectomy bed	Axial, coronal, sagittal	14 × 14–15 × 15	3,166–5,419/81–112	3/0 sp	256 × 256/2–3	90	
DWI single-shot EPI	Prostatectomy bed	Axial	20 × 20–22 × 22	2,650–5,000/81–82	5/0 sp	128 × 128/2		0, 600, 1,000
Dynamic contrast-enhanced imaging								
LAVA 3D fast gradient echo	Prostatectomy bed	Axial	14 × 14–15 × 15	5.9/2.7-10.1/2.5	3/50 % overlap	256 × 192/0.69–1.0	15	
Post–contrast-enhanced imaging								
LAVA 3D fast gradient echo	Entire pelvis	Axial	36 × 32.4–42 × 42	3.8–4.1/1.8	4–5/50 % overlap	320 × 224/0.7	15	

T1WI = T1-weighted imaging; FSE = fast spin echo; FRFSE = fast recovery fast sin echo; sp = interspace; DWI = diffusion-weighted imaging; EPI = echo planar imaging; T2WI = T2-weighted imaging; LAVA = liver acquisition with volume acceleration; LAVA Flex = LAVA with 2-point Dixon reconstruction; FSPGR = fast spoiled gradient echo.

TABLE 3
Probability Scores for Local Recurrence, Pelvic Nodal Metastasis, and Bone Metastasis on Per-Patient Basis and κ Interobserver Agreement

Observer per modality and site of recurrent disease	Probability Score					κ
	1	2	3	4	5	
Local recurrence (n = 115)						
MR imaging						
Observer 1	37	9	11	23	35	0.624
Observer 2	37	22	15	24	17	
^{11}C-choline PET/CT						
Observer 3	48	11	17	11	28	0.610
Observer 4	62	17	13	13	10	
Pelvic lymph nodal metastasis (n = 115)						
MR imaging						
Observer 1	57	7	17	14	20	0.563
Observer 2	51	16	18	22	8	
^{11}C-choline PET/CT						
Observer 3	60	6	5	4	40	0.702
Observer 4	58	5	5	18	29	
Intrapelvic bone metastasis (n = 115)						
MR imaging						
Observer 1	84	12	3	8	8	0.514
Observer 2	67	20	13	8	7	
^{11}C-choline PET/CT						
Observer 3	95	4	2	5	9	0.800
Observer 4	95	4	3	5	8	

spectively and independently reviewed ^{11}C-choline PET/CT images on a workstation (Advantage Workstation 4.4; GE Healthcare). Two board-certified genitourinary radiologists with 22 and 2 y of prostate MR imaging experience, who were masked to other information, retrospectively and independently reviewed multiparametric MR imaging on a PACS workstation (Centricity RA1000; GE Healthcare).

Diagnostic certainty when interpreting PET/CT and MR imaging was graded 1 (definitely absent), 2 (probably absent), 3 (indeterminate), 4 (probably present), and 5 (definitely present) for 3 different locations: locally recurrent tumor, pelvic LN metastases, and pelvic skeletal metastases. Focal ^{11}C-choline activity in the prostatectomy bed greater than adjacent background uptake and not due to excreted radiotracer in the urine was graded 4 or 5 regardless of corresponding structural abnormality. LNs were graded 4 or 5 if distinct focal activity on PET images coregistered to a visible LN on CT regardless of size; LNs distal to the mid external iliac chains were excluded because normal radiotracer activity in these regions is common (*12*). Focal skeletal sites of uptake above background marrow activity were graded 4 or 5 unless explanatory posttraumatic or degenerative change was evident. The 2 nuclear medicine radiologists also recorded the presence of extrapelvic metastatic lesions on ^{11}C-choline PET/CT in the same way. Semiquantitative analysis of the abnormal radiotracer uptake for each suspicious recurrent/metastatic lesion as well as background prostatectomy bed was performed using the maximum standardized uptake value (SUVmax).

The number, location, and both long- and short-axis dimensions of suspected locally recurrent and metastatic lesions on MR imaging were recorded. In scoring pelvic nodal status by MR imaging, the following diagnostic criteria were used: short-axis diameter of pelvic LN ≥ 10 mm (score, 5), 8–9.9 mm (score, 4), 5–7.9 mm (score, 3), 1–4.9 mm (score, 2), and not seen (score, 1). For region-specific comparisons, pelvic LNs were divided into 10 regions: right and left common iliac, external iliac, internal iliac/obturator, perivesical, and presacral regions.

Discordant readings by the 2 observers for each modality were resolved by subsequent consensus review.

Statistical Analysis

Interobserver agreement for MR imaging and PET/CT by location was determined on a per-patient basis. Interobserver agreement was considered to be slight when κ was less than 0.21, fair when κ ranged from 0.21 to 0.40, moderate when κ ranged from 0.41 to 0.60, substantial when κ ranged from 0.61 to 0.80, and almost perfect when κ was greater than 0.80.

To estimate each imaging modality's utility to diagnose intrapelvic recurrence of prostate cancer, receiver-operating-characteristic (ROC) analysis was used. A ROC contrast estimation was used to compare the diagnostic capability of MR imaging and PET/CT on a per-patient basis. To test whether the areas under the ROC curves (AUC) were different, the correlation of the testing methods was accounted for in the analysis. Tests for differences in sensitivity, specificity, and accuracy between imaging modalities were conducted with the McNemar test. To calculate the sensitivity and specificity of each modality, scores of 4 and 5 were considered positive. A P value of less than 0.05 was considered to indicate a statistically significant difference for all analyses. Statistical analysis was performed using SAS software (version 9.3; SAS Institute).

RESULTS

The characteristics of 115 patients and their original cancers are presented in Table 2.

The standard of reference (either positive or negative) for the diagnosis of local recurrence in the prostatectomy bed and pelvic

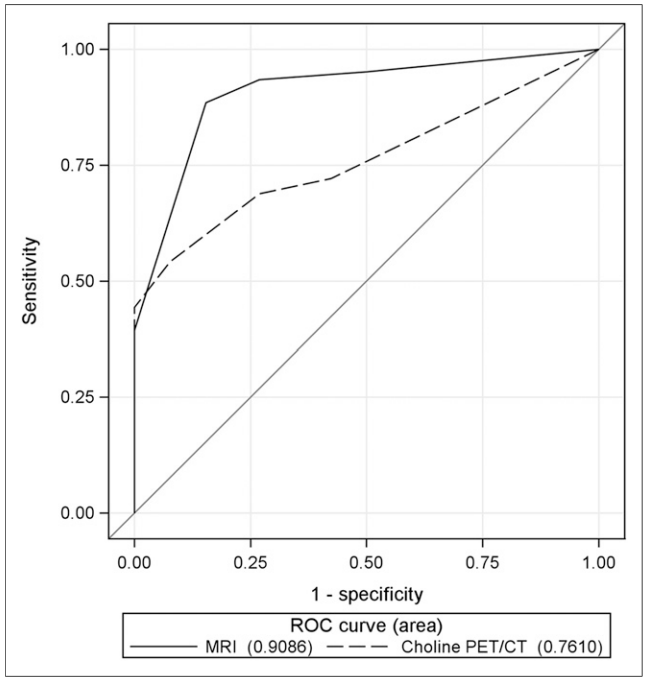

FIGURE 1. ROC curves generated for multiparametric MR imaging (solid line) and ^{11}C-choline PET/CT (dashed line) in depicting local recurrence in 87 postprostatectomy patients on per-patient basis. AUC calculated for multiparametric MR imaging of 0.9086 was significantly higher than that for ^{11}C-choline PET/CT of 0.7610 (P = 0.0079).

TABLE 4
Comparison of Diagnostic Performance of MR Imaging and ^{11}C-Choline PET/CT at 3 Scored Sites of Recurrent/Metastatic Disease on Per-Patient Basis

Modality per site of recurrent disease	Sensitivity	Specificity	Accuracy	AUC
Local recurrence (n = 87)				
MR imaging	88.5% (54/61*; 95% CI, 78.2%–94.3%)	84.6% (22/26; 95% CI, 66.5%–93.8%)	87.4% (76/870*; 95% CI, 78.8%–92.8%)	0.91* (95% CI, 0.85–0.97)
^{11}C-choline PET/CT	54.1% (33/61; 95% CI, 41.7%–66.0%)	92.3% (24/26; 95% CI, 75.9%–97.9%)	65.5% (57/87; 95% CI, 55.1%–74.7%)	0.76 (95% CI, 0.67–0.85)
Pelvic LN metastasis (n = 70)				
MR imaging	64.0% (32/50; 95% CI, 50.1%–75.9%)	85.0% (17/20; 95% CI, 64.0%–94.8%)	70.0% (49/70; 95% CI, 58.5%–79.5%)	0.81 (95% CI, 0.71–0.91)
^{11}C-choline PET/CT	90.0% (45/50*; 95% CI, 78.6%–95.7%)	100.0% (20/20; 95% CI, 83.9%–100%)	92.9% (65/70*; 95% CI, 84.3%–96.9%)	0.95* (95% CI, 0.91–1.00)
Pelvic bone metastasis (n = 95)				
MR imaging	87.5% (14/16; 95% CI, 64.0%–96.5%)	96.2% (76/79; 95% CI, 89.4%–98.7%)	94.7% (90/95; 95% CI, 88.3%–97.7%)	0.93 (95% CI, 0.84–1.00)
^{11}C-choline PET/CT	81.3% (13/16; 95% CI, 57.0%–93.4%)	98.7% (78/79; 95% CI, 93.2%–99.8%)	95.8% (91/95; 95% CI, 89.7%–98.4%)	0.90 (95% CI, 0.80–1.00)

*Statistically significant difference between MR imaging and ^{11}C-choline PET/CT ($P < 0.05$).
CI = confidence interval.

LN and skeletal metastases was met in 87, 70, and 95 patients, respectively. Documented positive locally recurrent disease and pelvic LN and bone metastases were present in 61 of 87 (70.1%), 50 of 70 (71.4%), and 16 of 95 (16.8%) patients, respectively. Seventy-nine patients had recurrence in only 1 of the 3 sites, 21 had recurrence in 2 sites, and 2 had recurrence in all 3 sites.

The PSA levels of the 87 patients who met the reference standard for determining the presence or absence of local recurrence ranged from 0.58 to 43.6 ng/mL, with a median of 4.44 ng/mL. The PSA levels of the 70 patients who met the reference standard with respect to pelvic LN metastasis ranged from 0.82 to 43.6 ng/mL, with a median PSA of 2.6 ng/mL. The PSA levels of the 95 patients who met the reference standard with respect to pelvic bone metastases ranged from 0.58 to 68.3 ng/mL, with a median PSA of 2.7 ng/mL.

Table 3 shows the results on a per-patient basis of the overall diagnostic confidence scores for the assessment of local recurrence and pelvic LN and bone metastases by each of the 2 readers for both the MR imaging and the PET/CT studies as well as interobserver agreement scores (k). All 6 assessments demonstrated interobserver agreements that were good (0.514–0.800).

Diagnostic Performance

Local Recurrence. In 61 of the 87 patients, local recurrence was documented by histopathologic findings at biopsy (n = 35), subsequent reduction in PSA level after salvage radiotherapy(n = 14), and clinical follow-up (n = 12). Sixteen patients were found to have no local recurrence by negative biopsy result and imaging follow-up.

The patient-based AUC, sensitivity, and accuracy of multiparametric MR imaging for detecting local recurrence were significantly better than that of PET/CT (P = 0.0079, < 0.0001, and 0.0004, respectively) (Fig. 1; Table 4). Among 61 patients with local recurrence, 32 patients (52.5%) were correctly diagnosed by both MR imaging and PET/CT (Fig. 2), 22 (36.1%) were correctly diagnosed by MR imaging only (Fig. 3), 6 (9.8%) were falsely negative by both modalities, and 1 (1.6%) was correctly diagnosed by PET/CT only (Table 5). Of 22 patients whose local

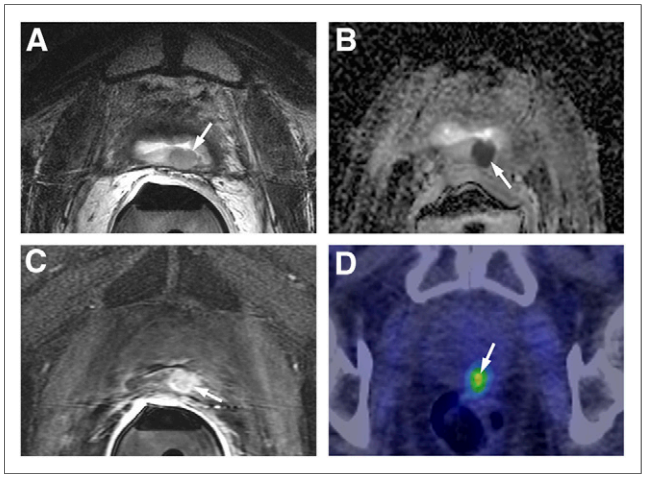

FIGURE 2. A 60-y-old man with PSA level of 6.3 ng/mL, who underwent RP for prostate carcinoma 3.2 y earlier and then received salvage external-beam radiotherapy and androgen-deprivation therapy. Results of concordant true-positive MR imaging and ^{11}C-choline PET/CT with score for both MR imaging and choline PET/CT of 5 for local recurrence are shown. (A) Axial T2-weighted MR image shows 10 × 11 mm, slightly hyperintense nodule in posterior bladder neck near vesicourethral anastomosis. (B and C) Corresponding areas of restricted diffusion on apparent diffusion coefficient map (arrow) (B) and hyperenhancement on DCE MR imaging (arrow) (C). (D) ^{11}C-choline PET/CT shows choline-avid lesion in prostatectomy bed, with SUVmax of 6.2 (arrow).

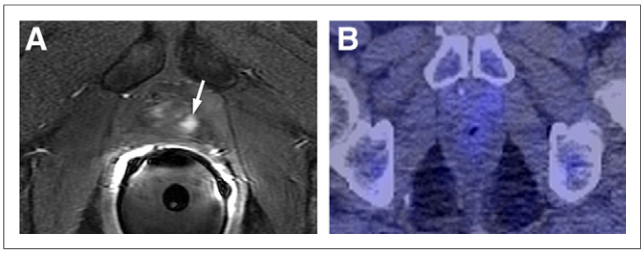

FIGURE 3. A 63-y-old patient with PSA level of 1.3 ng/mL, who underwent RP 10 y earlier and then received androgen-deprivation therapy. Results of discordant true-positive MR imaging and false-negative ^{11}C-choline PET/CT with a score for MR imaging of 5 and a score for ^{11}C-choline PET/CT of 1 for local recurrence are shown. (A) Hyperenhancing nodule (6 mm) in prostatectomy bed to left of vesicourethral anastomosis on DCE MR imaging (arrow), which appeared slightly hyperintense on T2-weighted imaging (not shown). There was no corresponding restricted diffusion on apparent diffusion coefficient map (not shown). (B) ^{11}C-choline PET/CT at corresponding level shows no focal area of choline uptake.

recurrence was detected by MR imaging only, 15 patients showed no abnormal extrapelvic findings on PET/CT, and the serum PSA values of these 15 patients ranged from 0.58 to 3.5 ng/mL, with a median PSA of 1.9 ng/mL.

The locations of a total of 66 locally recurrent lesions in 54 patients identified by MR imaging were perianastomotic (n = 39), seminal vesicle bed (n = 11), retrovesical or posterior bladder wall (n = 10), anterior or lateral surgical margins of the prostatectomy (n = 4), and vesicorectal angle (n = 2).

The short- and long-axis diameter of the 66 locally recurrent lesions detected by MR imaging ranged from 3 to 25 mm (mean, 10.2 mm) and from 4 to 36 mm (mean, 16.3 mm), respectively. For locally recurrent lesions with a short-axis diameter of 4 mm or less, between 5 and 9 mm, or 10 mm or greater, PET/CT had a detection sensitivity of 20% (1/5), 42.9% (12/28), and 81.8% (27/33), respectively.

The SUVmax of the 41 locally recurrent lesions in 33 patients correctly diagnosed by PET/CT ranged from 1.7 to 12.6, with a mean of 4.81. The SUVmax of the prostate bed in 28 patients

TABLE 5
Description of Discordant Findings and Concordant False-Negative Findings Between MR Imaging and ^{11}C-Choline PET/CT at 3 Scored Sites of Recurrent and Metastatic Disease

Region	Findings		No. of patients	Details
	MR imaging	^{11}C-choline PET/CT		
Local recurrence	TP	FN	22	The location of 26 lesions in 22 patients: perianastomotic (n = 16), retrovesical or bladder wall (n = 5), seminal vesicle bed (n = 3), and surgical margin (n = 2). Mean short-axis diameter of the 26 lesions: 7.5 ± 3.8 mm (range, 3– 20 mm). The SUVmax of the prostate bed in the 22 patients: mean, 2.00 ± 0.75 (range, 1.0–3.9).
	FN	TP	1	Perianastomotic location, with SUVmax of 2.4.
	TN	FP	2	SUVmax of 2.2 and 2.5, respectively.
	FP	TN	4	The locations of 4 lesions: perianastomotic (n = 1), bladder wall (n = 1), seminal vesicle bed (n = 1), and surgical margin (n = 1).
	FN	FN	5	The SUVmax of the prostatectomy bed in 5 patients: mean, 1.98 ± 0.94 (range, 0.9–3.1).
Pelvic LN metastases	FN	TP	13	The location of 15 LNs in the 13 patients were external iliac (n = 9), common iliac (n = 3), and internal iliac/internal obturator (n = 3). Mean short-axis diameter of the 15 LNs: 5.5 ± 1.3 mm (range, 3–7 mm). The SUVmax of the 15 lymph nodes: mean, 2.96 ± 1.26 (range,1.5–6.7).
	FP	TN	3	The locations of LNs: external iliac (n = 2) and common iliac (n = 1), measuring 8, 9, and 12 mm, respectively.
	FN	FN	5	The locations of LNs: external iliac (n = 2), internal iliac/internal obturator (n = 2), and common iliac (n = 1).
Pelvic bone metastases	TP	FN	3	Two of 3 patients had history of ADT: one had a sclerotic lesion, and the other had a mixed lytic and sclerotic lesion. Third patient had a sclerotic lesion with no history of hormone therapy.
	FN	TP	2	Lytic (n = 1) and sclerotic lesions (n = 1). The SUVmax was 3.4 and 5.3, respectively.
	FP	TN	3	Two of the 3 patients had history of ADT: sclerotic change in one and lytic change in the other. Degenerative change in a third patient.
	TN	FP	1	Physiologic uptake (SUVmax, 2.3) of the vertebra was overdiagnosed as abnormal.

TP = true-positive; FN = false-negative; TN = true-negative; FP = false-positive; ADT = androgen-deprivation therapy.

TABLE 6
Numbers of Local Recurrence and Body LN or Skeletal Metastases and Detection Rate of Those Lesions by MR Imaging and ^{11}C-Choline PET/CT Stratified by PSA Levels

PSA	*n*	No. of patients with LR	No. of patients with Mets	Sensitivity of MR imaging for LR	Sensitivity of choline PET/CT for LR	Sensitivity of choline PET/CT for Mets
<1	7	5	2	80.0% (4/5; 95% CI, 37.6%–96.4%)	20.0% (1/5; 95% CI, 3.6%–62.4%)	100% (2/2; 95% CI, 34.2%–100%)
1 ≤ <2	30	15	16	86.7% (13/15; 95% CI, 62.1%–96.3%)	53.3% (8/15; 95% CI, 30.1%–75.2%)	87.5% (14/16; 95% CI, 64.0%–96.5%)
2 ≤ <4	39	22	23	95.5% (21/22; 95% CI, 78.2%–99.2%)	45.5% (10/22; 95% CI, 26.9%–65.3%)	91.3% (21/23; 95% CI, 79.8%–100%)
4 ≤ <10	27	12	26	83.3% (10/12; 95% CI, 55.2%–95.3%)	75.0% (9/12; 95% CI, 46.8%–91.1%)	100% (26/26; 95% CI, 87.1%–100%)
10 ≤	12	7	12	85.7% (6/7; 95% CI, 48.7%–97.4%)	71.4% (5/7; 95% CI, 35.9%–91.8%)	83.3% (10/12; 95% CI, 55.2%–95.3%)
Total	115	61	79	88.5% (54/61; 95% CI, 78.2%–94.3%)	54.1% (33/61; 95% CI, 41.7%–66.0%)	92.4% (73/79; 95% CI, 86.6%–98.2%)

LR = local recurrence in prostatectomy bed; Mets = metastasis to both intra- and extrapelvic regions of body; CI = confidence interval.

FIGURE 4. ROC curves for multiparametric MR imaging (solid line) and ^{11}C-choline PET/CT (dashed line) in depicting pelvic LN metastasis in 70 postprostatectomy patients on per-patient basis. AUC calculated for ^{11}C-choline PET/CT of 0.9520 was significantly higher than that for multiparametric MR imaging of 0.8120 ($P = 0.0064$).

who were diagnosed as false-negative by ^{11}C-choline PET/CT ranged from 0.9 to 3.9, with a mean of 1.98. The background SUVmax of the prostatectomy surgical beds, which was measurable in 107 of the 117 patients, ranged from 0.9 to 3.0, with a mean of 1.57. In the other 10 cases, the background SUVmax could not be measured because of considerable overlap with tumor uptake.

The numbers of local recurrence and detection rate of those lesions by pelvic MR imaging and PET/CT as stratified by PSA levels are shown in Table 6. Choline PET/CT was substantially less sensitive in depicting locally recurrent tumor with lower PSA levels when compared with MR imaging.

Pelvic LN Metastasis. In 50 of the 70 patients, pelvic LN metastasis was documented by histopathologic findings at surgical lymphadenectomy ($n = 23$) and at CT-guided biopsy ($n = 5$) and clinical follow-up ($n = 22$). Twenty patients were found to have no LN metastasis by imaging follow-up.

The patient-based AUC, sensitivity, and accuracy of PET/CT for detecting pelvic nodal metastases were significantly better than those of MR imaging ($P = 0.0064$, 0.0003, and < 0.0001, respectively) (Figs. 4 and 5; Tables 4 and 5). PET/CT correctly detected 71 of the 90 areas of pelvic LN metastases, with these lesions demonstrating a mean SUVmax of 4.39 with a range of 1.6–8.7.

Twenty-three patients who were proved to have LN metastases by lymphadenectomy had 51 positive metastatic LN regions and 71 nonmetastatic LN regions. With PET/CT, the sensitivity, specificity, and accuracy for detecting pelvic metastatic LNs on a per-region analysis were 66.7% (34/51), 95.8% (68/71), and 83.6% (102/122), respectively, whereas the corresponding values for MR imaging were 39.2% (20/51), 94.4% (67/71), and 71.3% (87/122), respectively. The difference in sensitivity and accuracy between the 2 modalities was significant ($P = 0.001$ and 0.0006).

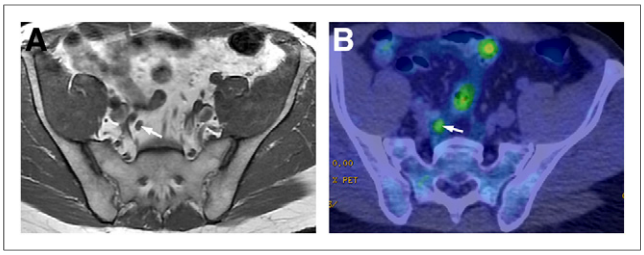

FIGURE 5. A 54-y-old man with PSA level of 2.7 ng/mL, who underwent RP 2.5 y earlier and then received salvage external-beam radiotherapy. Results for discordant false-negative MR imaging and true-positive ^{11}C-choline PET/CT with a score for MR imaging of 3 and a score for ^{11}C-choline PET/CT of 5 for LN metastasis are shown. (A) Axial T1-weighted MR image shows 5 × 7 mm right internal iliac LN (arrow). (B) ^{11}C-choline PET/CT image at corresponding level demonstrates choline-avid right internal iliac LN (arrow) with SUVmax of 3.8.

Pelvic Skeletal Metastasis. In 16 of the 95 patients, pelvic skeletal metastasis was confirmed by biopsy (n = 1) and clinical follow-up (n = 15). Seventy-nine patients were found to have no skeletal metastasis by imaging follow-up.

There was no statistical difference between MR imaging and PET/CT for patient-based AUC, sensitivity, specificity, or accuracy for detecting pelvic bone metastases (Figs. 6 and 7; Table 4). All false-positive (n = 3) and false-negative (n = 2) interpretations by MR imaging were correctly diagnosed by PET/CT, and conversely all false-positive (n = 1) and false-negative (n = 3) interpretations by PET/CT were correctly diagnosed by MR imaging (Table 5). The SUVmax of 19 pelvic metastatic bone lesions in the 16 patients detected by PET/CT ranged from 1.9 to 10.8, with a mean of 5.38.

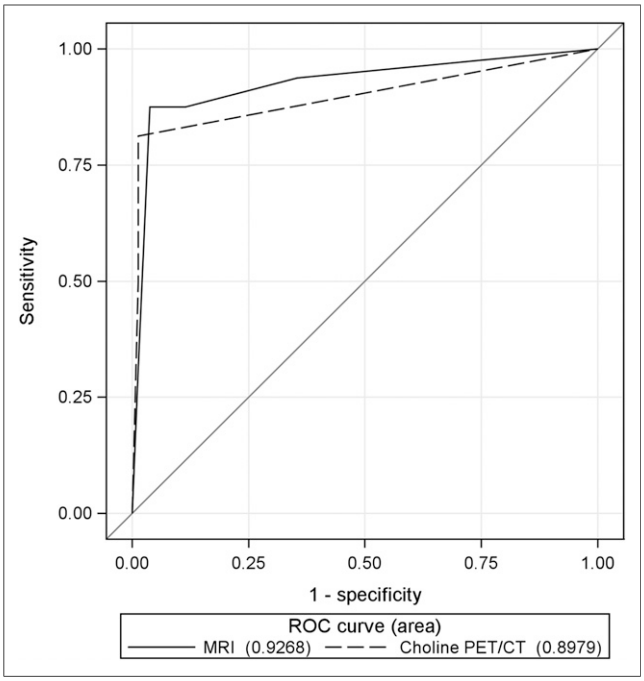

FIGURE 6. ROC curves for multiparametric MR imaging (solid line) and ^{11}C-choline PET/CT (dashed line) in depicting pelvic bone metastasis in 90 postprostatectomy patients on per-patient basis. AUC calculated for multiparametric MR imaging of 0.9268 was not significantly higher than that for ^{11}C-choline PET/CT of 0.8979 (P = 0.6897).

Body ^{11}C-Choline PET/CT Findings. Of the 115 patients, ^{11}C-choline PET/CT detected metastatic disease outside the pelvis in 34 of the 115 (29.6%), including 20 patients with extrapelvic LN metastases, 19 patients with extrapelvic bone metastases, and 2 patients with lung metastases. The PSA of these 34 patients ranged from 0.82 to 68.3 ng/mL, with a median PSA of 4.45 ng/mL. Patient-based analysis showed that the sensitivity, specificity, and accuracy of PET/CT for detecting body LN metastases in 78 patients were 91.4% (53/58), 100.0% (20/20), and 93.6% (73/78), respectively. Patient-based analysis showed that the sensitivity, specificity, and accuracy of PET/CT for detecting body bone metastases in 100 patients were 90.6% (29/32), 98.5% (67/68), and 96.0% (96/100), respectively. Patient-based analysis showed that the sensitivity, specificity, and accuracy of PET/CT for detecting body LN or bone metastases in 96 patients were 92.3% (72/78), 100.0% (18/18), and 93.8% (90/96), respectively.

The numbers of lymph nodal or skeletal metastases in the body and detection rate of those lesions by PET/CT according to PSA levels are also shown in the Table 6. Choline PET/CT remained sensitive in depicting lymph nodal and skeletal metastases in patients with lower PSA levels.

Of note, PET/CT incidentally detected advanced lung cancer with mediastinal and hilar LN metastases in 1 patient.

DISCUSSION

Our analysis of 115 patients with rising PSA after RP for prostate carcinoma who underwent both multiparametric MR imaging and ^{11}C-choline PET/CT demonstrated a complementary role of the 2 modalities in depicting recurrent disease, with 3 important findings. First, multiparametric MR imaging had excellent sensitivity and accuracy for the detection of locally recurrent tumors in the prostate bed superior to PET/CT. Second, PET/CT had excellent sensitivity and accuracy for the diagnosis of LN metastases superior to MR imaging. Third, PET/CT and MR imaging demonstrated equally excellent accuracy for the diagnosis of pelvic bone metastases and played a complementary role in cases of false-negatives by either modality. Overall, in the instances of discordant results between the 2 modalities, the MR imaging results should be strongly favored for interpretation of local recurrence whereas PET/CT results should be strongly favored for the interpretation of LN metastases.

The diagnosis of local recurrence after RP is often challenging. Transrectal ultrasound–guided biopsy of the prostatic fossa is traditionally the procedure of choice. However, it is invasive, is costly, and has a relatively low but not insignificant rate of complications such as infection. Its yield is suboptimal in patients with low PSA levels (*13*). A negative biopsy result does not exclude local recurrence because of potential sampling error, and repeated biopsies are often required. As reported in the literature (*6–9*) and confirmed in our series, the current gold standard for diagnosing locally recurrent prostate cancer after RP is dynamic gadolinium contrast-enhanced MR imaging with endorectal coil. MR imaging is considered a valid tool in evaluating patients with suspected local recurrence. MR imaging is also the most accurate for clearly defining the morphology of the local recurrence, in terms of size, location, and relationship to critical structures such as sphincters (*14*). With the increasing use of more focused, salvage therapies in locally recurrent prostate cancer,

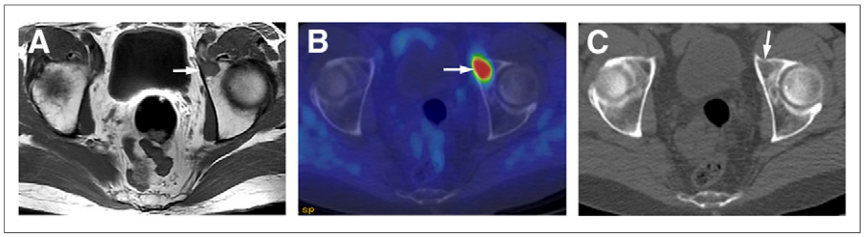

FIGURE 7. A 68-y-old man with PSA level of 5.0 ng/mL, who underwent RP 3 y earlier and then received salvage external-beam radiotherapy and androgen-deprivation therapy. Results for concordant true-positive MR imaging and ^{11}C-choline PET/CT results with a score for both MR imaging and ^{11}C-choline PET/CT of 5 for skeletal metastasis are shown. (A) Axial T1-weighted image shows 13-mm enhancing lesion in anterior left acetabulum (arrow). (B) ^{11}C-choline PET/CT image demonstrates corresponding choline-avid lesion (arrow) with SUVmax of 6.4. (C) Unenhanced CT scan of 7B shows subtle asymmetric lytic process (arrow).

this detailed information by MR imaging is invaluable. However, MR imaging is only moderately sensitive in detecting pelvic LN metastases.

In our series, the detectability of local recurrence by PET/CT falls short of this goal, with a limited sensitivity of 54% and accuracy of 66%, because of the limited spatial resolution of the current generation of PET scanners, which is approximately 7 mm. Even for lesions exceeding 7 mm, the negative effects of partial-volume averaging become increasingly stronger as lesion size diminishes. Souvatzoglou et al. (*5*) showed that only 7 (19%) of 37 patients who were referred for salvage radiotherapy to the prostatectomy bed because of PSA failure (PSA range, 0.3–1.8 ng/mL) had increased choline uptake in the prostatectomy bed with PET/CT. Panebianco et al. (*9*) compared multiparametric MR imaging and ^{18}F-choline PET/CT for detecting local recurrence after RP in 84 patients and confirmed the superiority of MR imaging, notably in patients with smaller lesions and low PSA. In the same study, the difference was larger in group A (lesion size range, 5–7 mm; PSA level range, 0.8–1.4 ng/mL) than in group B (lesion size range, 7.6–19.4 mm; PSA level range, 1.3–2.5 ng/mL); the AUCs of MR imaging and PET/CT were 0.833 and 0.562 in group A and 0.971 and 0.837 in group B, respectively.

The evaluation of LN metastases is crucial in restaging patients with PSA failure after RP. In a study of 25 prostatectomy patients with PSA failure using pelvic and retroperitoneal lymphadenectomy histopathology results as reference (*15*), sensitivity, specificity, positive predictive value, negative predictive value, and accuracy of ^{11}C-choline PET/CT in depicting LN metastases were 100%, 66%, 90%, 100%, and 92% for patient-based analysis and 64%, 90%, 86%, 72%, and 77% for lesion-based analysis. The low negative predictive value for lesion-based analysis indicates the limited performance of ^{11}C-choline PET/CT to detect microscopic nodal metastasis whereas the high positive predictive value represents an important result to facilitate appropriate treatment.

PET/CT, acquiring both metabolic and anatomic imaging data, can evaluate the body in a single examination. Many authors have demonstrated that ^{11}C-choline PET/CT is useful for restaging prostate cancer after RP, although the performance of PET/CT is clearly dependent on the PSA level (*2,3*). Picchio et al. (*16*) noted that the positive detection rate using choline PET/CT improves with increasing PSA values, but the routine use of choline PET/CT for restaging prostate cancer after RP cannot be recommended for PSA values less than 1 ng/mL. Because the disease site in patients with mildly elevated PSA values is most frequently local, multiparametric MR imaging with dynamic contrast enhancement is the preferred imaging examination of choice in this setting rather than ^{11}C-choline PET/CT.

This study has several limitations. It was a retrospective study in a single institution. There may have been a patient selection bias for patients who were clinically evaluated with both MR imaging and ^{11}C-choline PET/CT, given the relatively high rate of positive cases. Most patients in our series had at least 1 focus of recurrent or metastatic disease, with relatively high PSA levels, and were at higher risk for recurrent disease with a higher prevalence of advanced pathologic features at RP, and only a minority of patients was documented to be free of local recurrence or distant metastasis. A histologic examination in all patients would have been optimal, but that was not possible in all patients for practical and ethical reasons. Instead of a lesion-based analysis of LN metastases, region- and patient-based comparisons were made between imaging and surgical pathologic findings in this retrospective study. Fusion between PET/CT and MR imaging findings was entirely visual and cognitive.

CONCLUSION

Pelvic multiparametric MR imaging performance with endorectal coil is superior in prostatectomy patients in depicting local prostate bed recurrence whereas ^{11}C-choline PET/CT offers an advantage in detecting metastatic disease to LN and bone in high-risk patients. The combination of multiparametric MR imaging and ^{11}C-choline PET/CT provides the best comprehensive assessment for restaging in prostatectomy patients with suspected locally recurrent or metastatic disease.

DISCLOSURE

The costs of publication of this article were defrayed in part by the payment of page charges. Therefore, and solely to indicate this fact, this article is hereby marked "advertisement" in accordance with 18 USC section 1734. No potential conflict of interest relevant to this article was reported.

REFERENCES

1. Cookson MS, Aus G, Burnett AL, et al. Variation in the definition of biochemical recurrence in patients treated for localized prostate cancer: the American Urological Association Prostate Guidelines for Localized Prostate Cancer Update Panel report and recommendations for a standard in the reporting of surgical outcomes. *J Urol.* 2007;177:540–545.
2. Castellucci P, Fuccio C, Nanni C, et al. Influence of trigger PSA and PSA kinetics on ^{11}C-choline PET/CT detection rate in patients with biochemical relapse after radical prostatectomy. *J Nucl Med.* 2009;50:1394–1400.
3. Giovacchini G, Picchio M, Coradeschi E, et al. Predictive factors of [^{11}C]choline PET/CT in patients with biochemical failure after radical prostatectomy. *Eur J Nucl Med Mol Imaging.* 2010;37:301–309.
4. Reske SN, Blumstein NM, Glatting G. [^{11}C]choline PET/CT imaging in occult local relapse of prostate cancer after radical prostatectomy. *Eur J Nucl Med Mol Imaging.* 2008;35:9–17.
5. Souvatzoglou M, Krause B, Pürschel A, et al. Influence of ^{11}C-choline PET/CT on the treatment planning for salvage radiation therapy in patients with biochemical recurrence of prostate cancer. *Radiother Oncol.* 2011;99:193–200.

6. Cirillo S, Petracchini M, Scotti L, et al. Endorectal magnetic resonance imaging at 1.5 Tesla to assess local recurrence following radical prostatectomy using T2-weighted and contrast-enhanced imaging. *Eur Radiol.* 2009;19: 761–769.
7. Boonsirikamchai P, Kaur H, Kuban DA, Jackson E, Hou P, Choi H. Use of maximum slope images generated from dynamic contrast-enhanced MRI to detect locally recurrent prostate carcinoma after prostatectomy: a practical approach. *AJR.* 2012;198:W228–236.
8. Wassberg C, Akin O, Vargas HA, Shukla-Dave A, Zhang J, Hricak H. The incremental value if contrast-enhanced MRI in the detection of biopsy-proven local recurrence of prostate cancer after radical prostatectomy: effect of reader experience. *AJR.* 2012;199:360–366.
9. Panebianco V, Sciarra A, Lisi D, et al. Prostate cancer: 1HMRS-DCEMR at 3T versus [^{18}F]choline PET/CT in the detection of local prostate cancer recurrence in men with biochemical progression after radical retropubic prostatectomy (RRP). *Eur J Radiol.* 2012;81:700–708.
10. Hara T, Kosaka N, Kishi H. Development of ^{18}F-fluoroethylcholine for cancer imaging with PET: synthesis, biochemistry, and prostate cancer imaging. *J Nucl Med.* 2002;43:187–199.
11. Luboldt W, Küfer R, Blumstein N, et al. Prostate carcinoma: diffusion-weighted imaging as potential alternative to conventional MR and ^{11}C-choline PET/CT for detection of bone metastases. *Radiology.* 2008;249:1017–1025.
12. Murphy RC, Kawashima A, Peller PJ. The utility of ^{11}C-choline PET/CT for imaging prostate cancer: a pictorial guide. *AJR.* 2011;196:1390–1398.
13. Deliveliotis C, Manousakas T, Chrisofos M, Skolarikos A, Delis A, Dimopoulos C. Diagnostic efficacy of transrectal ultrasound-guided biopsy of the prostatic fossa in patients with rising PSA following radical prostatectomy. *World J Urol.* 2007;25:309–313.
14. Sella T, Schwartz LH, Swindle PW, et al. Suspected local recurrence after radical prostatectomy: endorectal coil MR imaging. *Radiology.* 2004;231:379–385.
15. Scattoni V, Picchio M, Suardi N, et al. Detection of lymph-node metastases with integrated [^{11}C]choline PET/CT in patients with PSA failure after radical retropubic prostatectomy: results confirmed by open pelvic-retroperitoneal lymphadenectomy. *Eur Urol.* 2007;52:423–429.
16. Picchio M, Briganti A, Fanti S, et al. The role of choline positron emission tomography/computed tomography in the management of patients with prostate-specific antigen progression after radical treatment of prostate cancer. *Eur Urol.* 2011;59:51–60.